Int. J. Heat Mass Transfer. Vol. 8, pp. 621–638. Pergamon Press 1965. Printed in Great Britain

DEVELOPED LAMINAR FLOW HEAT TRANSFER FROM AIR FOR VARIABLE PHYSICAL PROPERTIES

D. BRADLEY
Mechanical Engineering Department, University of Leeds
and
A. G. ENTWISTLE
Central Electricity Generating Board, Portishead

(*Received* 6 *January* 1964 *and in revised form* 14 *August* 1964)

Abstract—The effect of the variation of specific heat, density, viscosity and thermal conductivity with temperature, is investigated theoretically for developed air flow cooling in a circular tube. Numerical solutions are presented which were obtained using a digital computer and are for a range of air temperatures from 350 to 2500°K.

The momentum and energy equations are considered and numerical solutions of temperature and velocity profiles, Nusselt number and pressure drop coefficient are given for different mixed mean temperatures.

Solutions are presented for the conditions of:

1. All axial temperature gradients at fixed radius equal to the bulk temperature gradient.
2. Constant wall temperature.

In addition to showing the effects of property variation, the solutions show also that the effect of axial conduction becomes important at low Reynolds number and that the effect of axial momentum change can be considerable for large temperature differences between air and wall. For vertically upward flow the effect of gravitational force is studied and numerical solution indicates a flow reversal near the wall at a lower value of Gr/Re than in the uniform property solution.

NOMENCLATURE

c, mean specific heat at constant pressure between T_w and T;

c_m, mean specific heat at constant pressure between T_w and T_m;

$\dot{c}$, specific heat at constant pressure at temperature T;

f, friction coefficient;

F, pressure drop coefficient, defined by (13);

g, acceleration due to gravity;

G, mass rate of flow through tube;

Gr, Grashof number $= \dfrac{8 r_w^3 \rho_m^2 g(T_m - T_w)}{T_m \mu_m^2}$, for a perfect gas;

h, enthalpy/unit mass, measured above wall temperature, at radius r;

k, thermal conductivity at radius r;

Nu, Nusselt number $= \dfrac{2 \alpha r_w}{k_m}$;

p, pressure;

r, radius;

r_w, tube radius;

R, dimensionless radius $= \dfrac{r}{r_w}$;

Re, Reynolds number $= \dfrac{2 u_m r_w \rho_m}{\mu_m}$;

T, absolute temperature at radius r;

T_m, mixed mean temperature (abs.) or bulk temperature;

T_w, wall temperature (abs.);

u, velocity at radius r;

u_m, mean velocity defined by (4);

U, dimensionless velocity $= \dfrac{u}{u_m}$;

$\bar{U}$, velocity parameter defined by (9);

x, axial distance along tube;

X, dimensionless axial distance $= x/r_w$.

Greek symbols

α, heat-transfer coefficient;

θ, dimensionless temperature $= \dfrac{T - T_w}{T_m - T_w}$;

μ, viscosity at radius r;

ρ, density at radius r.

Subscripts

m, mean condition. Properties evaluated at mixed mean temperature, T_m;

w, condition at tube wall.

INTRODUCTION

THE laminar flow of a fluid with heat transfer in a circular tube has been analysed by many workers. The basic differential equation for conservation of energy for such flow, the Fourier–Poisson equation, was first correctly derived by Poisson [1] in 1835. Solutions of the equation obtained by Graetz in 1883–1885 are summarized by Drew [2]. The first solution of Graetz was for an axial velocity unchanging with radius and the second, more practical, solution was for a parabolic velocity profile with respect to radius, as given by Poiseuille's equation. Both solutions were for uniform wall temperature. Graetz obtained a temperature profile and a heat-transfer coefficient in the form of infinite series of which the first three terms were evaluated. In 1956 Sellars, Tribus and Klein [3] gave a formula for calculating all the eigenvalues and eigenfunctions, not only for the condition of uniform wall temperature, but also of uniform wall heat flux and of linear wall temperature.

All these solutions give the "thermal boundary layer" development in the axial direction. The analyses share the following assumptions:

1. Fluid specific heat, conductivity, viscosity and density independent of temperature.
2. Effects of gravitational force and varying density (free convection) neglected.
3. Axial conduction and momentum change neglected.
4. Energy dissipation due to viscosity neglected.
5. No radial component of velocity.
6. Symmetry about tube axis.

Analysis of the problem is simplified in the region where the velocity and thermal boundary layers have become fully developed, where there is no radial component of velocity and where the dimensionless velocity and temperature profiles are unchanging with axial distance. This is the situation at distances beyond the "entry length" and is called the region of fully developed flow.

Experiments revealed departures from the Graetz analysis and Colburn [4] ascribed these to viscosity variation with temperature, causing in developed flow a deviation from Poiseuille's parabolic velocity profile, and also, at lower Reynolds numbers, to natural convection. By introducing a viscosity ratio and the Grashof number into non-dimensional relationships the experimental results could be empirically correlated. The same phenomena also explained departures of the fluid friction factor from the isothermal value.

Attempts have been made to explain the deviations from "isothermal" solutions by theoretical analysis using the momentum and energy equations. Early work allowed separately for viscosity variations and for density variations. Pigford [5] summarizes these attempts and gives solutions allowing both for variation in viscosity and for variation in density in the gravitational field. His analysis is for high flow rates in short vertical tubes with uniform wall temperature.

Deissler [6] has allowed for variations of viscosity, density and thermal conductivity with temperature in fully developed flow. He derives theoretical velocity and temperature profiles, friction parameters and Nusselt numbers for gases and liquid metals at different ratios of bulk temperature to wall temperature. The wall boundary condition is that of constant temperature difference between fluid at a given radius and wall, irrespective of axial distance. For constant property values this is the uniform heat flux condition. Diessler makes assumptions (2), (3), (4), (5), and (6) listed above and also that the specific heat is constant.

It should be noted that the concept of developed flow is somewhat altered as a consequence of property variations. The velocity and temperature profiles continue to change even after the complete development of the two boundary layers. Developed flow under these conditions is taken to mean the state of affairs where both boundary layers, which begin to build up at the

walls at entry to the tube, have extended across the full diameter, notwithstanding some continuing change in the profiles. It is no longer strictly true to equate the radial velocity component to zero. However, because this velocity is usually small compared with the axial component there is, in such cases, no great error in analyses based on developed flow, with no radial velocity. Hallman [7] presents some experimental evidence which supports the local use of the results of heat-transfer analyses on the basis of such a fully developed flow model.

Free convection effects have been investigated theoretically by Ostroumov [8], Hallman [9] and Hanratty, Rosen and Kabel [10]. These investigators solve the momentum and energy equations allowing for density variation in the gravitational field, simplification being achieved by analysing the uniform heat flux condition with developed flow. All fluid properties except the density are assumed constant and any radial component of velocity is neglected. The analyses demonstrate the distortion of velocity and temperature profiles due to free convection. Scheele, Rosen and Hanratty [11] carried out experimental studies of the transition to disturbed flow in vertical tubes and Hallman [7] obtained experimental values of Nusselt numbers and also noted the development of instabilities.

The mathematical investigation of Singh [12] extends the Graetz, uniform wall temperature, solution for Poiseuille flow by allowing for the effect of axial heat conduction, as well as energy dissipation due to viscosity and internal heat generation. Singh found that for constant properties the effect of axial conduction was almost negligible for Peclet numbers greater than 100. The range of Peclet numbers from 1 to 100 for uniform heat flux and constant property values has been analysed numerically by Petukhov and Tsvetkov [13].

Despite extensive investigations of laminar flow heat transfer in circular tubes, it is seen that recourse always has been made to some of the assumptions (1–6) listed previously. The present authors' interest in the problem arises from studies on hot freshly burnt gases flowing at low Reynolds numbers in cooled, uniform temperature, tubes. Under these conditions, the variation of fluid properties with temperature clearly is significant, as is free convection and, possibly, also axial conduction and change of momentum. It was therefore necessary to carry out the present analyses for this combination of circumstances. Information on the properties of gases is not, in general, available throughout the temperature range of interest. Data on the properties of air, however, are available in the range 250 to 2500°K and it was decided to use these data in the analysis as this would provide a guide to the behaviour of other hot gases. The property values used are those listed by Eckert and Drake [14] and shown graphically in Fig. 1, supplemented by values of enthalpy taken from Hilsenrath [15].

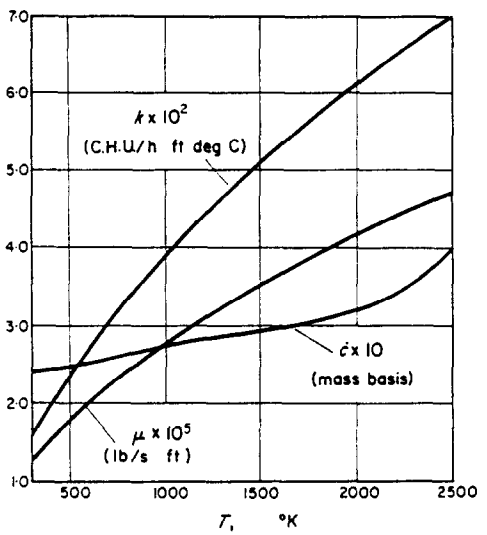

FIG. 1. Conductivity, viscosity and specific heat of air as functions of temperature at atmospheric pressure.

A complete solution of the problem is a matter of great complexity even with the aid of digital computers and has not, as yet, been accomplished. The neglect of any radial component of velocity introduces considerable mathematical simplification and is the most restrictive assumption which has been made in deriving the results presented by the present authors. These are presented not as complete solutions but as a contribution towards a fuller understanding of the problem. Velocity and temperature profiles, Nusselt numbers and pressure drop coefficients have been evaluated numerically for a range of

conditions in developed flow using the Ferranti Pegasus computer at Leeds University.

The different influences are shown by the presentation of solutions under four headings:

a. Uniform temperature gradient solutions.
b. Uniform enthalpy profile, and uniform wall temperature solutions.
c. Free convection effects.
d. Axial conduction and momentum change effects.

ANALYSIS

The essentials of the analysis are the derivation of the velocity profile from the momentum equation and of the temperature profile from the energy equation. These profiles are then able to yield the pressure drop coefficient and the Nusselt number.

Assumptions

It is assumed that flow is steady, axisymmetric, and that the energy dissipation due to viscosity may be neglected. The equation of the state of the fluid is that of a perfect gas with ρ proportional to p/T.

It is further assumed that the flow is fully developed with no radial component of velocity. Usually this velocity would be very much smaller than the axial velocity and this assumption is justified, but this is not so at very low flow rates.

The numerical results which are presented are derived from the momentum and energy equations without recourse to the continuity equation $\partial u\rho/\partial x = 0$. It is found that, having obtained the velocity and temperature profiles, this last equation is not fully satisfied. The reason for this inconsistency lies in the neglect of any radial velocity. Allowance for this would produce somewhat more accurate solutions but at the expense of a considerable increase in mathematical complexity. The continuity equation does not imply that the axial momentum change on the left-hand side of the momentum equation (1), below, is necessarily negligible.

Momentum equation

The cases of vertically upward flow with cooling of the gas is analysed. The Navier–Stokes equation, allowing for axial changes of momentum and for gravitational force opposing motion, is given in polar coordinates by

$$\rho u \frac{\partial u}{\partial x} = -\rho g - g\left(\frac{\partial p}{\partial x}\right) + \frac{4}{3}\left(\frac{\partial \mu\,(\partial u/\partial x)}{\partial x}\right) + \frac{1}{r}\left(\frac{\partial \mu r\,(\partial u/\partial r)}{\partial r}\right), \tag{1}$$

$(\partial p/\partial r) = 0$ and boundary conditions are;

$$r = 0 \quad (\partial u/\partial r) = 0 \tag{2}$$

$$r = r_w \quad u = 0 \tag{3}$$

Define a mean velocity of flow given by

$$u_m = (G/\pi r_w^2\, \rho_m) \tag{4}$$

and a Reynolds number

$$Re = \frac{2\, u_m\, r_w\, \rho_m}{\mu_m} = \frac{2G}{\mu_m\, \pi\, r_w} \tag{5}$$

$Re\mu_m$ is constant along the tube length.

As $(Gr/Re) = 2\, r_w\, g\,(T_m - T_w)/\, u_m^2\, T_m$ (1) gives

$$\frac{U}{u_m}\left(\frac{\partial u}{\partial X}\right) = -\left[\left(\frac{Gr}{Re^2}\right)\left(\frac{T_m}{2(T_m - T_w)}\right)\right] - \left[\left(\frac{4\,\rho_m^2\, g}{\rho\,\mu_m^2\, Re^2}\right)\left(\frac{\partial p\, r_w^2}{\partial X}\right)\right] + \left[\left(\frac{8\,\rho_m}{3\,u_m\,\rho\,\mu_m}\right)\frac{1}{Re}\left(\frac{\partial \mu(\partial u/\partial X)}{\partial X}\right)\right] + \left[\left(\frac{2\,\rho_m}{\mu_m\, Re\,\rho\, R}\right)\left(\frac{\partial \mu\, R\,(\partial U/\partial R)}{\partial R}\right)\right]. \tag{6}$$

Integrating with respect to R between the limits $R = 0$ and $R = R$ and using (2) in the dimensionless form gives,

$$\left(\frac{\partial U}{\partial R}\right) = \left[\left(\frac{\rho_m g R}{\mu_m Re\,\mu}\right)\left(\frac{\partial p\, r_w^2}{\partial X}\right)\right] + \left[\left(\frac{T_m^2 \mu_m}{4(T_m - T_w)}\right)\frac{Gr}{Re}\left(\frac{\int_0^R (R/T)\,.\,dR}{\mu R}\right)\right]$$
$$+ \left[\left(\frac{Re\,\mu_m T_m}{2}\right)\left(\frac{\int_0^R (UR/Tu_m)(\partial u/\partial X)\,dR}{\mu R}\right)\right] - \frac{4}{3}\left[\frac{\int_0^R (R/u_m)\left(\partial\mu \dfrac{\partial u}{\partial X}\Big/\partial X\right).dR}{\mu R}\right]. \quad (7)$$

Integrating again with respect to R between the limits $R = 1$ and $R = R$ and using (3) in the dimensionless form gives,

$$U = \left[\frac{\rho_m g}{\mu_m Re}\frac{\partial p\, r_w^2}{\partial X}\int_1^R \frac{R}{\mu}\cdot dR\right] + \left[\frac{T_m^2 \mu_m}{4(T_m - T_w)}\frac{Gr}{Re}\int_1^R \frac{\int_0^R (R/T)\,.\,dR}{\mu R}\cdot dR\right] +$$

$$\left[\frac{Re\,\mu_m T_m}{2}\int_1^R \frac{\int_0^R (UR/Tu_m)(\partial u/\partial X)\,.\,dR}{\mu R}\cdot dR\right] - \frac{4}{3}\int_1^R \frac{\int_0^R (R/u_m).[\partial\mu\,(\partial u/\partial X)/\partial X]\,.\,dR}{\mu R}\cdot dR \quad (8)$$

In the derivation of numerical solutions it is convenient to introduce a parameter

$$\bar{U} = -\,[2u/(\partial p/\partial x)\, r_w^2 g] \quad (9)$$

and

$$\bar{U}_m = -\,[2\,u_m/(\partial p/\partial x)\, r_w^2 g]. \quad (10)$$

Clearly

$$U = (\bar{U}/\bar{U}_m).$$

From (4) and (9)

$$\bar{U}_m = \left[\left(-2\int_0^{r_w} 2\pi r\, u\rho\, dr\right)\Big/\left(\pi r_w^2\, \rho_m \frac{\partial p}{\partial x} r_w^2 g\right)\right] = 2\,T_m \int_0^1 \frac{\bar{U}R}{T}\cdot dR. \quad (11)$$

In terms of the parameter $\bar{U}$, (8) becomes

$$\bar{U} = -\int_1^R \frac{R}{\mu}\cdot dR + \frac{\bar{U}_m T_m^2 \mu_m}{4(T_m - T_w)}\cdot\frac{Gr}{Re}\int_1^R \frac{\int_0^R (R/T)\,.\,dR}{\mu R}\cdot dR +$$

$$\bar{U}_m \int_1^R \left(\frac{\dfrac{Re\,\mu_m T_m}{2}\displaystyle\int_o^R \frac{UR}{Tu_m}\cdot\frac{\partial u}{\partial X}\cdot dR - \frac{4}{3}\int_o^R \frac{R}{u_m}\frac{\partial\mu\,(\partial u/\partial x)}{\partial X}\cdot dR}{\mu R}\right) dR. \quad (12)$$

Pressure drop coefficient, F

This defines the pressure drop in the most general case, when allowance is made for viscosity, free convection and axial momentum change. In analyses where free convection and axial momentum change are neglected and where the pressure change is due to viscosity alone, then F is the same as the more widely used friction coefficient, f. This is true in the solutions presented under headings (a) and (b) below.

Let

$$\frac{\partial p}{\partial x} = -\frac{F\,\rho_m\,u_m^2}{r_w\,g} \tag{13}$$

Equations (5), (10) and (13) give

$$F = \frac{4}{\bar{U}_m\,Re\,\mu_m} \tag{14}$$

Energy equation

This is

$$\frac{\partial kr\,(\partial T/\partial r)}{\partial r} + r\frac{\partial k\,(\partial T/\partial x)}{\partial x} = u\,\rho r\frac{\partial h}{\partial x} \tag{15}$$

Boundary conditions are

$$r = 0 \quad \frac{\partial T}{\partial r} = 0 \tag{16}$$

$$r = r_w \quad T = T_w \tag{17}$$

Integrating (15) twice with respect to r, between the limits shown, gives

$$T_w - T = \int_r^{r_w} \frac{\int_0^r \left(u\,\rho r\frac{\partial h}{\partial x} - r\frac{\partial k\,(\partial T/\partial x)}{\partial x}\right) \mathrm{d}r}{kr}\,\mathrm{d}r \tag{18}$$

Let enthalpies be measured above a datum temperature equal to T_w. The mixed mean temperature, T_m, is defined by

$$T_m - T_w = \frac{\int_0^{r_w} (c/c_m)\,\rho u\,2\pi r\,(T - T_w)\,.\,\mathrm{d}r}{G} \tag{19}$$

Substituting (18) in (19) gives

$$T_m - T_w = -\int_0^{r_w} \frac{\frac{c}{c_m}\,\rho u\,2\pi r\left\{\int_r^{r_w} \frac{\int_0^r \{u\,\rho\,r\,(\partial h/\partial x) - r\,[\partial k\,(\partial T/\partial x)/\partial x]\}\,\mathrm{d}r}{kr}\cdot \mathrm{d}r\right\}\mathrm{d}r}{G} \tag{20}$$

Consideration of the boundary conditions and introduction of the heat-transfer coefficient yields:

$$\alpha\,(T_w - T_m)\,2\pi\,r_w + 2\pi\int_0^{r_w} \frac{\partial kr\,(\partial T/\partial x)}{\partial x}\cdot \mathrm{d}r = G\frac{\partial h_m}{\partial x} \tag{21}$$

From (20) and (21)

$$\alpha = \frac{\{(\int_0^{r_w} \rho u\,2\pi r\,\mathrm{d}r)^2 - [(2\pi\int_0^{r_w} \rho u\,2\pi r\,\mathrm{d}r)/(\partial h_m/\partial x)]\,([\int_0^{r_w} kr\,(\partial T/\partial x)]/\partial x)\,.\,\mathrm{d}r\}}{\left\{2\pi r_w\int_0^{r_w}(c/c_m)\,\rho u\,2\pi r\left[\int_r^{r_w}(\int_0^r \{[u\rho r\,(\partial h/\partial x)/\partial h_m/\partial x] - [r/(\partial h_m/\partial x)][\partial k\,(\partial T/\partial x)/\partial x]\}\,\mathrm{d}r/kr)\,.\,\mathrm{d}r\right]\right\}\mathrm{d}r} \tag{22}$$

The mean value of all temperature dependent properties is the value at temperature T_m.

Introducing dimensionless parameters and with ρ proportional to p/T (22) gives

$$\alpha r_w/k_m = \frac{[\int_0^1 (UR/T).\mathrm{d}R]^2 - \{[2\int_0^1 (UR/T).\mathrm{d}R]/(T_m Re\,\mu_m)(\partial h_m/\partial X)\}\{\int_0^{r_w} R.[\partial k\,(\partial T/\partial X)/\partial X].\mathrm{d}R\}}{\int_0^1 (c/c_m)(UR/T)\left(\left\{\int_R^1 [\int_0^R ((UR/T).[(\partial h/\partial X)/(\partial h_m/\partial X)] - 2R/[T_m Re\,\mu_m(\partial h_m/\partial X)][\partial k\,(\partial T/\partial X)/\partial X])\,\mathrm{d}R]/(kR/k_m)\right\}.\mathrm{d}R\right)\mathrm{d}R} \tag{23}$$

It has been demonstrated by Knudsen and Katz [16] that a triple integral of the type in the denominator of (23) is equivalent to one of the type in the denominator of (24), below

$$Nu = 2\alpha r_w/k_m = \frac{2[\int_0^1 (UR/T).\mathrm{d}R]^2\,(1 - \{2\int_0^1 R.[\partial k\,(\partial T/\partial X)/\partial X].\mathrm{d}R\}/[T_m Re\,\mu_m(\partial h_m/\partial x).\int_0^1 (UR/T).\mathrm{d}R])}{\left\{\int_0^1\left[\int_0^R (c/c_m)(UR/T)\,\mathrm{d}R\int_0^R \{[(UR/T)(\partial h/\partial X)/(\partial h_m/\partial X)] - [2R/T_m Re\,\mu_m(\partial h_m/\partial X)][\partial k\,(\partial T/\partial X)/\partial X]\}.\mathrm{d}R\right]\Big/(k/k_m)R\right\}.\mathrm{d}R} \tag{24}$$

Temperature profile

From (18) and (21)

$$T_w - T = 2\pi\left(\{\alpha(T_w - T_m)r_w + \int_0^{r_w} R[\partial k\,(\partial T/\partial x)/\partial x].\mathrm{d}r\}/G\right)\left\{\int_r^{r_w}\left[\int_0^r ([u\rho r\,(\partial h/\partial x)/(\partial h_m/\partial x)] - r[\partial k\,(\partial T/\partial x)/\partial x]/(\partial h_m/\partial x))\,\mathrm{d}r\right]\Big/kr\right\}.\mathrm{d}r \tag{25}$$

Whence

$$T_w - T = \left[\frac{\alpha(T_w - T_m)r_w + \int_0^1 R.[\partial k\,(\partial T/\partial X)/\partial X].\mathrm{d}R}{\int_0^1 (UR/T).\mathrm{d}R}\right] \times \int_R^1 \frac{\int_0^R \{(UR/T).[(\partial h/\partial X)/(\partial h_m/\partial X)] - (2R/T_m Re\,\mu_m)([\partial k\,(\partial T/\partial X)/\partial X]/(\partial h_m/\partial X))\}.\mathrm{d}R}{kR}.\mathrm{d}R \tag{26}$$

In terms of the velocity parameter $\bar{U}$, (24), becomes,

$$Nu = \frac{2\left(\int_0^1 \frac{\bar{U}R}{T}\mathrm{d}R\right)^2\left[1 - \frac{4}{Re\,\mu_m(\partial h_m/\partial X)}\int_0^1 \frac{R\partial k\,(\partial T/\partial X)}{\partial X}\mathrm{d}R\right]}{\int_0^1\left[\int_0^R \frac{c}{c_m}\frac{\bar{U}R}{T}\mathrm{d}R\int_0^R\left(\frac{\bar{U}R}{T}\frac{\partial h/\partial X}{\partial h_m/\partial X} - \frac{4R}{Re\,\mu_m(\partial h_m/\partial X)}\cdot\frac{\partial k\,(\partial T/\partial X)}{\partial X}\cdot\int_0^1 \frac{\bar{U}R}{T}.\mathrm{d}R\right)\mathrm{d}R\Big/(k/k_m)R\right].\mathrm{d}R} \tag{27}$$

and (26) becomes

$$T_w - T = \left[\frac{\alpha r_w (T_w - T_m) + \int_0^1 R[\partial k (\partial T/\partial X)/\partial X] \cdot \mathrm{d}R}{\int_0^1 (\bar{U}R/T)\,\mathrm{d}R}\right] \times \int_R^1 \frac{\int_0^R \left\{(\bar{U}R/T).[(\partial h/\partial X)/(\partial h_m/\partial X)] - 4\dfrac{\int_0^1 (\bar{U}R/T)\,\mathrm{d}R \,.\, R\,[\partial k\,(\partial T/\partial X)/\partial X]}{Re\,\mu_m\,(\partial h_m/\partial X)}\right\}\mathrm{d}R}{kR} \cdot \mathrm{d}R. \quad (28)$$

Method of solution

A temperature profile is assumed for a particular mixed mean temperature and a particular wall temperature. $\bar{U}$ is evaluated from (12), the value of μ being appropriate to the temperature. $\bar{U}_m$ is found from (11) and $Re \times F$ from (14). The Nusselt number may now be found from (27), with values of enthalpy, specific heat and conductivity appropriate to the temperature. With this value of Nusselt number a new temperature profile may be derived from (28). The cycle is repeated and convergence usually occurs to solutions of sufficient accuracy after about four iterations.

Property values given in references [14] and [15] are for atmospheric pressure. The pressure dependence of these has been neglected. Special aspects of solutions are discussed under the four separate headings of numerical results and in the Appendix.

NUMERICAL RESULTS

(*a*) *Uniform temperature gradient solutions*

The condition is that $(\partial T/\partial x) =$ constant, at all radii. The primary purpose of these solutions is to reveal the temperature dependence of friction coefficient, Nusselt number and temperature and velocity profiles. Gravitational forces and axial momentum and conduction changes are neglected. With these conditions (12) becomes,

$$\bar{U} = -\int_1^R \frac{R}{\mu} \cdot \mathrm{d}R, \quad (12a)$$

(27) becomes

$$Nu = 2\left[\int_0^1 (\bar{U}R/T)\,\mathrm{d}R\right]^2 \Bigg/ \int_0^1 \left\{\frac{\int_0^R (c/c_m)\,.\,(\bar{U}R/T)\,\mathrm{d}R \int_0^R (\bar{U}R/T)\,(\dot{c}/\dot{c}_m)\,\mathrm{d}R}{R\,(k/k_m)}\right\}.\mathrm{d}R \quad (27a)$$

and (28) becomes

$$T_w - T = \frac{\alpha r_w (T_w - T_m)}{\int_0^1 (\bar{U}R/T)\,\mathrm{d}R} \int_R^1 \frac{\int_0^R (\bar{U}R/T)\,(\dot{c}/\dot{c}_m)\,\mathrm{d}R}{kR} \cdot \mathrm{d}R \quad (28a)$$

$\bar{U}_m$ is found from (11) and $Re\,F$ from (14).

For these conditions the pressure drop coefficient is equivalent to the conventional friction coefficient.

$Re \times F$ and Nu at different mixed mean temperatures, T_m, for wall temperatures, T_w, of 350, 700 and 1000°K are shown in Figs. 2 and 3. The isothermal values are 16 and 4·36 respectively. Typical velocity and temperature profiles are shown in Figs. 4 and 5 for $T_w = 350$°K and different

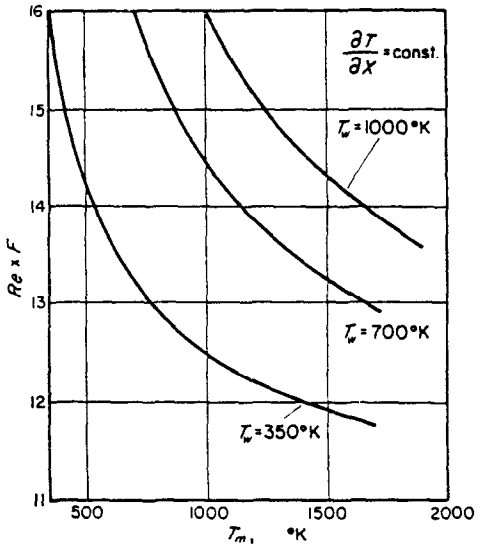

FIG. 2. Variation of pressure drop coefficient with mixed mean air temperature, for different wall temperatures.

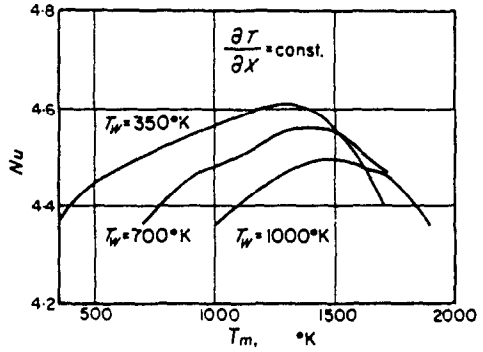

FIG. 3. Variation of Nusselt number with mixed mean air temperature, for different wall temperatures.

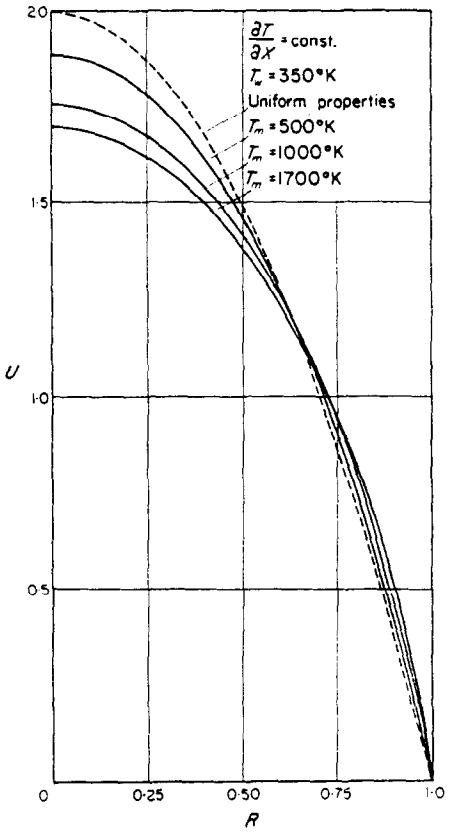

FIG. 4. Velocity profiles for different mixed mean air temperatures.

values of T_m. The isothermal parabolic velocity profile and the constant property temperature profile are shown for comparison.

(b) Uniform enthalpy profile and uniform wall temperature solutions

Gravitational forces and axial momentum and conduction changes again are neglected. $\bar{U}$ is given by (12a), (27) becomes

$$Nu = \frac{2\left[\int_0^1 (\bar{U}R/T)\,\mathrm{d}R\right]^2}{\int_0^1 \left\{\int_0^R ((c/c_m)(\bar{U}R/T)\,\mathrm{d}R \int_0^R (\bar{U}R/T)\,[(\partial h/\partial X)/(\partial h_m/\partial X)]\cdot \mathrm{d}R)/(k/k_m)\right\}\cdot \mathrm{d}R} \tag{27b}$$

and (28) becomes,

$$T_w - T = \frac{\alpha r_w (T_w - T_m)}{\int_0^1 (\bar{U}R/T)\,\mathrm{d}R} \int_R^1 \frac{\int_0^R (\bar{U}R/T)[(\partial h/\partial X)/(\partial h_m/\partial X)]\,.\,\mathrm{d}R}{kR} \cdot \mathrm{d}R \tag{28b}$$

The enthalpy profile is first assumed unchanged with axial distance: i.e. (h/h_m) at a particular radius is independent of X. This yields $(\partial h/\partial X)/(\partial h_m/\partial X) = h/h_m$.

With this simplifying condition the iterative process evaluates the Nusselt number and velocity and temperature profiles for given values of T_w and T_m. Solutions are obtained in this way for a series of values of T_m with a particular value of wall temperature, T_w.

Uniform wall temperature solutions are derived by evaluating from these temperature profiles a second set of values of $(\partial h/\partial X)/(\partial h_m/\partial X)$, without the uniform enthalpy profile restriction. This yields a further set of values of the ratio and a rapid convergence occurs to the uniform wall temperature solutions. The uniform enthalpy profile condition is thus a stage in the derivation of the more practical uniform wall temperature solutions.

For all these conditions the pressure drop coefficient is equivalent to the conventional friction coefficient. $Re \times F$ and Nu for different values of T_m and with $T_w = 350°K$ are shown in Figs. 6 and 7 for the three conditions so far imposed. Values of $Re \times F$ are identical for both the uniform enthalpy profile and the uniform wall temperature conditions. Velocity and temperature profiles with $T_w = 350°K$ and $T_m = 1400°K$ for the cases of uniform temperature gradient and uniform wall temperature are given in Figs. 8 and 9. The isothermal velocity profile is shown chain dotted in

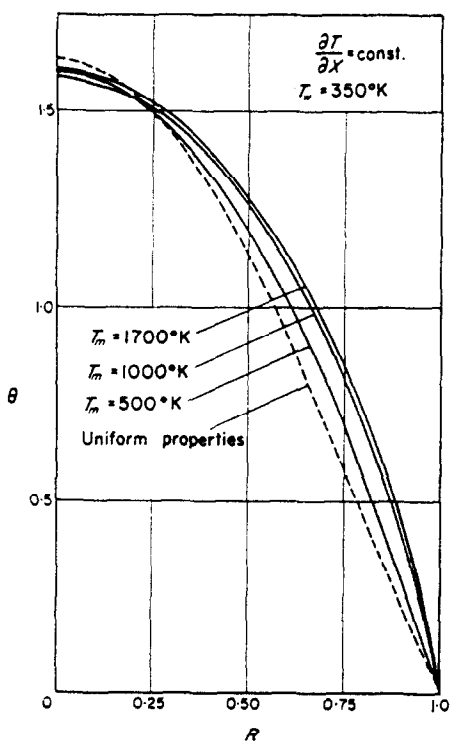

FIG. 5. Temperature profiles for different mixed mean air temperatures.

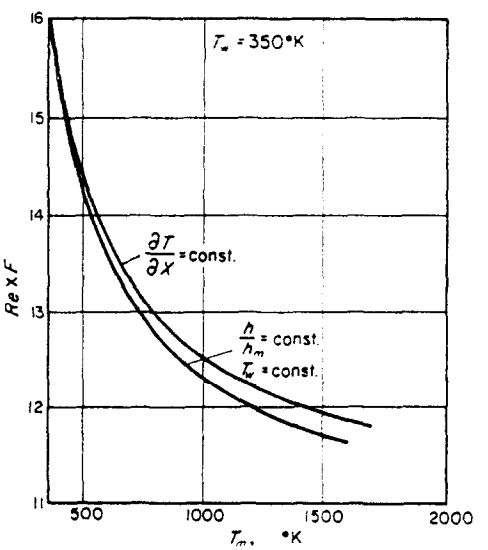

FIG. 6. Effect of boundary conditions on pressure drop coefficient.

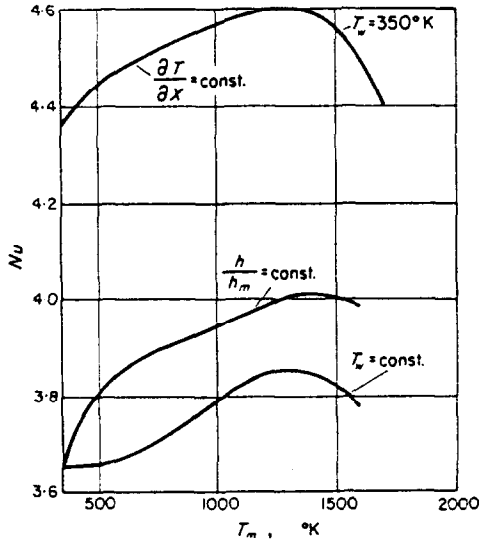

FIG. 7. Effect of boundary conditions on Nusselt number.

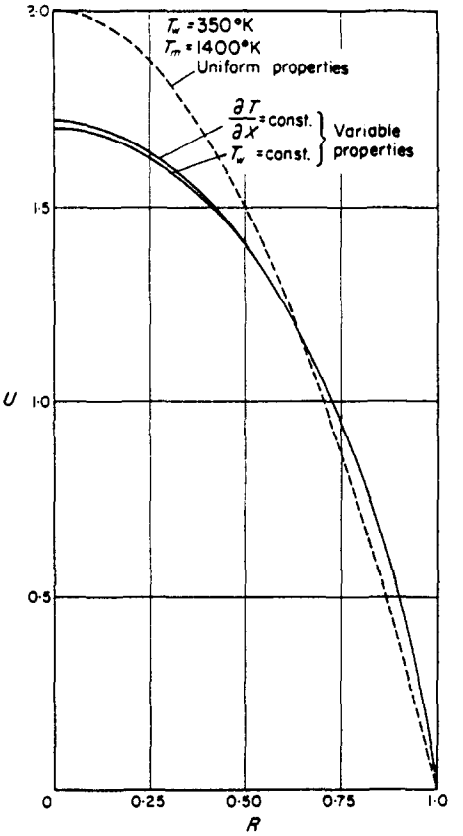

FIG. 8. Velocity profiles for different boundary conditions.

Fig. 8 and the uniform property temperature profiles for the two cases are shown chain dotted in Fig. 9.

(*c*) *Free convection effects*

Solutions with the uniform wall temperature condition are presented for different values of Gr/Re. Axial momentum and conduction changes are neglected. Equation (12) becomes

$$\bar{U} = -\int_1^R (R/\mu)\,.\,dR + \{\bar{U}_m\, T_m^2\, \mu_m/[4\,(T_m - T_w)]\}\,(Gr/Re) \int_1^R \{[\int_0^R (R/T)\,dR]/\mu R\}\,.\,dR \qquad (12c)$$

Nu is given by (27b) and $(T_w - T)$ by (28b).

In deriving solutions for given values of each of T_w, T_m and Gr/Re it is necessary first to assume a value of $\bar{U}_m$ in addition to the temperature profile. From (12c) a velocity profile is obtained and from (11) a new value of $\bar{U}_m$. Nu and a new temperature profile are derived and with the new value of $\bar{U}_m$ and temperature profile the cycle of computation is repeated. A number of iterations produces the final solutions. The uniform wall condition is approached via the uniform enthalpy profile condition, as outlined in Section (b).

$Re \times F$ is found from (14) and the values of this and of Nu are shown for different values of Gr/Re with $T_w = 350°K$ and $T_m = 1400°K$ in Fig. 10. The effect of free convection on the velocity and temperature profiles is shown by the full lines in Figs. 11 and 12. Two profiles are shown, one when no free convection is present, $Gr/Re = 0$, and the other with a contribution of free convection indicated by $Gr/Re = 40$.

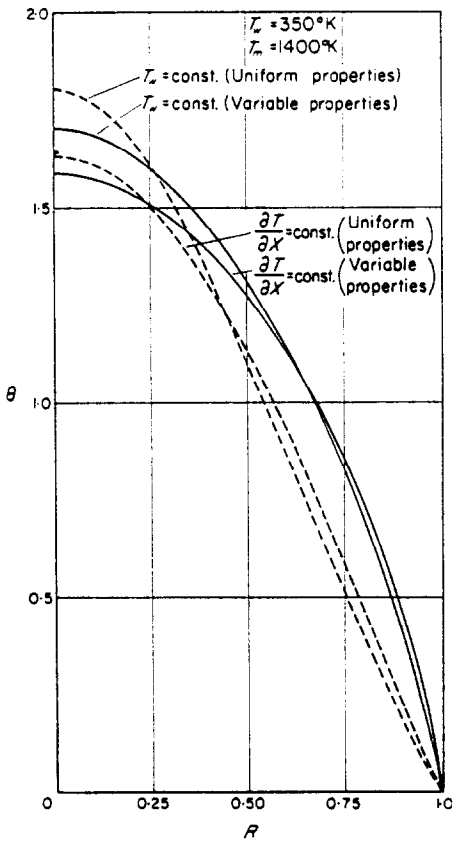

FIG. 9. Temperature profiles for different boundary conditions.

(d) Axial conduction and momentum change effects

So far axial gradient terms involving $\partial u/\partial X$ and $\partial T/\partial X$ have been neglected. These terms are evaluated from the velocity and temperature profiles and values of Nusselt number, derived for the conditions of uniform wall temperature with axial momentum and conduction changes neglected. Equation (21), with no axial conduction, gives

$$X_1 - X_0 = (Re\mu_m/2) \times \int_{T_m = T_{m0}}^{T_m = T_{m1}} [dh_m/Nu\, k_m\, (T_w - T_m)] \quad (21d)$$

This yields the relationship between mixed mean temperature, T_m, and axial distance, X. Gradient terms are evaluated from finite difference expressions using the computer.

Consider the valuation of (i), $(1/u_m)\,\partial u/\partial X$ and

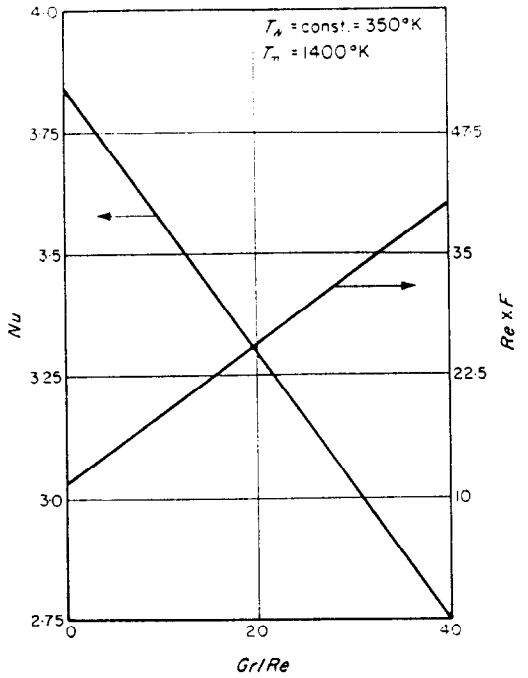

FIG. 10. Effect of Grashof:Reynolds number ratio on Nusselt number and pressure drop coefficient.

(ii) $(1/u_m)\,[\partial\mu\,(\partial u/\partial X)/\partial X]$, which appear in equation (12).

$$\frac{1}{u_m}\frac{\partial u}{\partial X} = \frac{\partial U}{\partial X} + \frac{U}{u_m}\frac{\partial u_m}{\partial X}$$

$$= \frac{\partial U}{\partial X} + \frac{U\pi r_w^2 \rho_m}{G}\,\frac{\partial (G/\pi r_w^2 \rho_m)}{\partial X}, \text{ from (4)}$$

$$= \frac{\partial U}{\partial X} + U\rho_m \frac{\partial (1/\rho_m)}{\partial X}$$

In laminar flow of high temperature gases the change in density is predominantly due to changes in temperature, changes in pressure being relatively small. For gases obeying the perfect gas equation of state

$$\frac{1}{u_m}\frac{\partial u}{\partial X} = \frac{\partial U}{\partial X} + \frac{U}{T_m}\frac{\partial T_m}{\partial X} = \phi \quad \text{, say (29)}$$

$$\frac{1}{u_m}\frac{\partial \mu\,(\partial u/\partial X)}{\partial X} = \frac{1}{u_m}\frac{\partial \mu\, u_m \phi}{\partial X}$$

$$= \rho_m \frac{\partial \mu\,(\phi/\rho_m)}{\partial X} = \frac{1}{T_m}\frac{\partial \mu\, T_m \phi}{\partial X} = \beta \quad \text{, say (30).}$$

ϕ and β are found for each value of R.

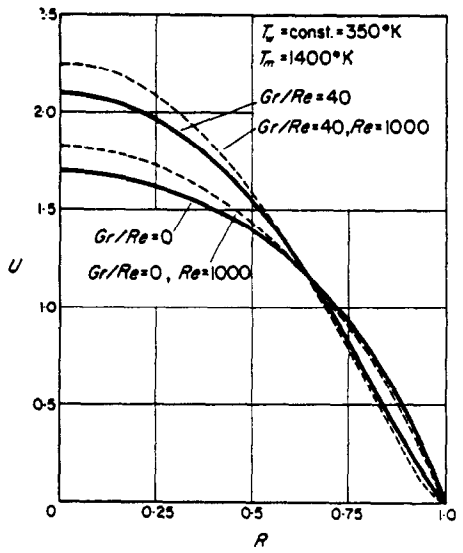

FIG. 11. Velocity profiles for different Reynolds and Grashof numbers.

In (12) the term in ϕ is more significant than that in β.

The terms in $\partial k\,(\partial T/\partial X)/\partial X$, $\partial h/\partial X$ and $\partial h_m/\partial X$ in equations (27) and (28) are evaluated without difficulty.

In deriving the uniform wall temperature solutions for a given value of each of T_w, T_m and Gr/Re a value of $\bar{U}_m$ must be first assumed along with a temperature profile. Equation (12) gives a velocity profile and (11) a new value of $\bar{U}_m$. Equation (27) gives Nu and (28) gives a new temperature profile. The cycle of computation may be repeated if necessary.

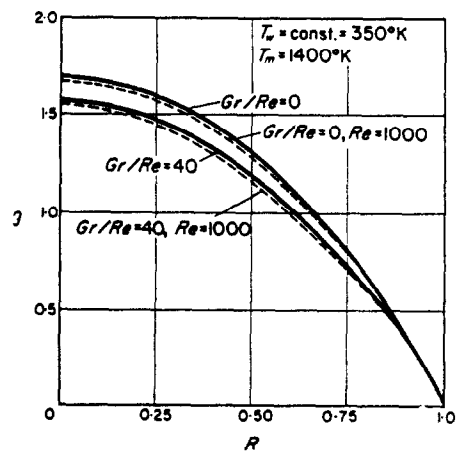

FIG. 12. Temperature profiles for different Reynolds and Grashof numbers.

With values of Nu obtained in this way it is possible to re-determine the axial gradient terms from (21). This was not necessary however for the range of values of Re presented here.

Typical effects of axial momentum and conduction upon velocity and temperature profiles are shown by the broken curves in Figs. 11 and 12, applicable to $Re = 1000$, $T_w = 350°K$, $T_m = 1400°K$ and $Gr/Re = 0$ and 40. With $Gr/Re = 0$, $Nu = 3{\cdot}84$, disregarding axial effects, and $Nu = 3{\cdot}80$ allowing for them, with $Re = 1000$. Corresponding values of $Re \times F$ are 11·79 and 1·34. The axial momentum effect is more significant than the conduction effect.

The effect of a variation in Reynolds number is shown for some typical conditions in Table 1. It will be seen that there is negligible change in value of Nu and $Re \times F$. There is little change in the velocity and temperature profiles.

Table 1. Effect of Reynolds number allowing for axial conduction and momentum change

$T_w = 350°K$ (const.), $T_m = 600°K$, $Gr/Re = 0$.

Re	1000	100	50
Nu	3·70	3·70	3·70
$Re \times F$	6·04	6·02	5·98

For comparison it should be noted that if no allowance is made for axial conduction and momentum change and the analysis is of the type described under heading (*b*), above, for constant wall temperature, then the values of Nu and $Re \times F$ for the temperatures of Table 1 are 3·67 and 13·46 respectively. For this analysis pressure change is due to viscosity alone and $F = f$.

The dependence of Nu and $Re \times F$ upon Gr/Re with $Re = 50$ is shown in Fig. 13.

DISCUSSION

The results show that over a wide range of temperature in which the properties of air vary considerably the value of the Nusselt number, evaluated with a conductivity equal to that at the mixed mean temperature, is surprisingly steady. For the conditions presented in Fig. 7

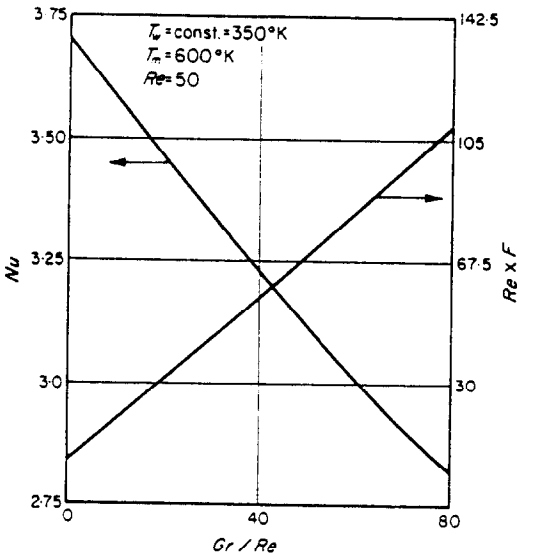

FIG. 13. Effect of Grashof:Reynolds number ratio on Nusselt number and pressure drop coefficient, with allowance for axial conduction and momentum change.

the maximum variation in the value of Nu for the uniform temperature gradient and the uniform wall temperature conditions is 5·7 per cent of the lowest, constant property, value. It is demonstrated also how the different imposed conditions give different solutions. Experimental support for the constancy of the value of Nu at the lower temperature ratios, T_m/T_w, for the uniform wall temperature condition is given by Kays and Nicoll [17]. These workers investigated the cooling of air for comparable wall temperature and for temperature ratios up to 1·79 and found negligible change in Nu. It is also of interest that for air heating the values of local Nusselt numbers along the entry length are close to those predicted by constant property analysis and this state of affairs probably extends to air cooling.

Nusselt numbers for the uniform temperature gradient condition, presented in Fig. 3, are shown in Fig. 14 as a function of T_w and temperature ratio. Deissler [6] expressed Nu as a function of this ratio and the relationship is shown by the broken curve. The maximum value of temperature ratio given by Deissler is 1·67 and the present analysis reveals that at higher values of this ratio the value of Nu decreases.

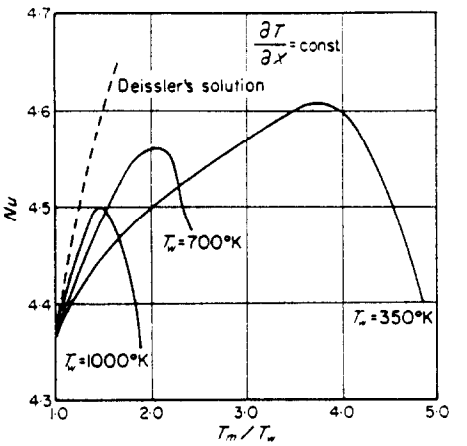

FIG. 14. Variation of Nusselt number with temperature ratio at different wall temperatures.

The uniformity in the value of Nu does not extend to the velocity and temperature profiles, where there are significant deviations from the constant property profiles. In Fig. 6 the product of Reynolds number and pressure drop coefficient shows a marked variation with temperature, but is not so dependent upon the imposed boundary condition. Figure 15 shows $Re \times F$ for the uniform temperature gradient condition as a function of temperature ratio. It should be noted

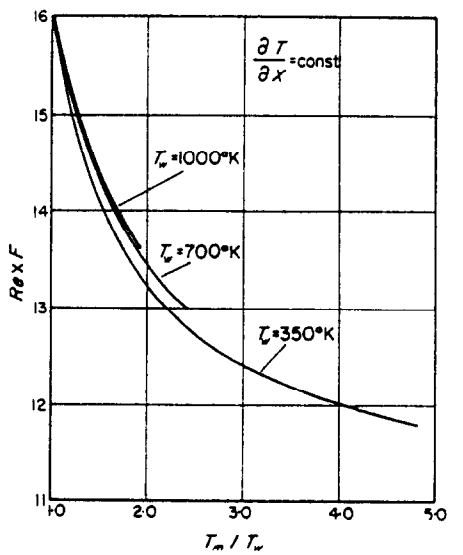

FIG. 15. Variation of friction coefficient with temperature ratio at different wall temperatures.

that in the results shown in Figs. 6 and 15 the pressure drop coefficient, F, is the same as the friction coefficient, f. The values correlate well, with little dependence upon wall temperature. Values calculated from Deissler's results lie close to the $T_w = 350°$ curve up to temperature ratios of 1·67.

The axial momentum change arising from the decreasing velocity of the cooling gas has important effects. Although a decrease in Re creates a greater rate of decrease of velocity with distance the decrease in mass rate of flow results in the momentum change being unaltered. Thus the effect of axial velocity gradients is almost independent of the actual value of Re. The axial momentum change gives rise to a force opposing motion, a change in velocity profile and a decrease in the value of $Re \times F$. Because of the more rapid cooling at larger temperature differences these effects are more marked at higher temperature ratios. The changes in temperature profile and in the value of Nu are not as striking.

At very low Reynolds numbers with large temperature differences the neglect of radial velocity in the analysis becomes less justifiable. It is of interest to note that the reduction in the value of $Re \times F$, as a result of the allowance for axial gradients, is not due to a breakdown in the assumed model, for the reduction occurs with a value of $Re = 1000$ when the neglect of radial velocity is justifiable. For low values of Reynolds number and large temperature differences there is a need to carry out a fuller analysis to ascertain the effects of radial velocity.

Allowance for axial conduction in the theory presented here does not produce very different results in the laminar range down to $Re = 50$. This is not to say that axial conduction may be neglected. For consider a cross section of the tube at right angles to the flow and another cross section, parallel and a very small distance away. The energy transfer by axial conduction into the thin disc formed by these sections ranges from 0·005 per cent of the total net energy transfer for $Re = 1000$ to 2·07 per cent at $Re = 50$, with $T_w = 350°$K and $T_m = 600°$K. The axial conduction as a percentage of the total net energy transfer at different Reynolds numbers is shown in Fig. 16. In the experimental determination of Nu allowance for axial conduction

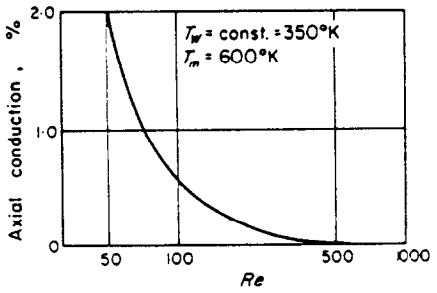

FIG. 16. Axial conduction as a proportion of net energy transfer at different Reynolds numbers.

becomes more important as Re is reduced. This is in line with the findings of Petukhov and co-workers [13], [18], who found allowance for axial conduction important in experimental work on liquid metals at Peclet numbers less than 160. This corresponds to $Re < 240$ for air at 600°K. Singh [12] found axial conduction to be of importance for Peclet numbers less than 100.

The decrease of Nu associated with an increase in the free convection effect, indicated by an increase in the value of Gr/Re, is in accord with the constant property solutions of Hanratty and co-workers [10]. Allowance for gravitational force increase the pressure drop and the product $Re \times F$ increases with Gr/Re, at constant Reynolds number. The pressure drop is dependent upon a complex of factors involving the viscous stress at the wall, the gravitational force and the momentum change. These interact and the use of a pressure drop coefficient seems more appropriate than a summation of supposedly separate influences.

Free convection does not have a significant effect upon the temperature profile but the effect observed on the velocity profile is of a fundamental interest. The denser gas close to the wall is retarded and the velocity profile deformed, as shown in Fig. 11. Ultimately a reversal of flow occurs close to the wall. In experimental studies using dye in water Scheele, Rosen and Hanratty [11] showed that a symmetrical downward flow at the wall develops. A further small increase in Gr/Re creates an asymmetric condition and there follows a sudden transition to eddying flow. This transition to turbulence, occurring at a laminar flow Reynolds number, enhances the

heat transfer. Scheele and Hanratty [19] introduce a dimensionless parameter, which can be shown equal to $Nu\,Gr/8\,Re$, as a measure of the free convection effect. Their theoretical analysis for the conditions of uniform properties and uniform heat flux shows zero velocity gradient to be attained at the wall when $Nu\,Gr/8\,Re = 52{\cdot}2$. Experiments with water show a transition to unsteady motion at $Nu\,Gr/8\,Re = 59$. Taking the appropriate value of Nu from reference [10], the critical value of Gr/Re for zero velocity gradient at the wall is 114. The analysis presented in the present paper gives zero velocity gradient when $Gr/Re = 72$, with $T_m = 600°K$, $T_w = 350°K$ and $Re = 50$ and the profile is shown in Fig. 17. Because of the onset of unsteady motion the results of the analysis with $Gr/Re > 72$ are not of practical value.

In seeking an explanation for the difference in the critical value of Gr/Re obtained by the two analyses, an examination of the velocity profiles in Fig. 8 reveals that the two different boundary conditions produce the same velocity gradient near the wall. A comparison of this with the uniform property gradient shown in the same figure shows that property variation is a factor which runs counter to flow reversal. Figure 11 reveals that the axial momentum change increases the tendency to flow reversal due to free convection.

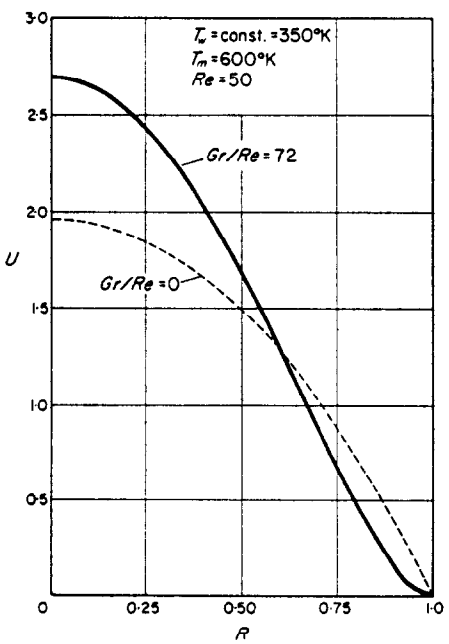

FIG. 17. Velocity profiles (i) neglecting gravitational force; and (ii) at critical value of Gr/Re.

CONCLUSIONS

1. With a value of conductivity appropriate to the mixed mean temperature there is less than 6 per cent variation in Nusselt number over a wide range of temperature ratios.
2. There is a greater variation with temperature in the value of the product of the Reynolds number and pressure drop coefficient. There is good correlation of this product with temperature ratio, with little dependence upon wall temperature, as shown in Fig. 15.
3. Variation of physical properties causes considerable deviation from the uniform property velocity and temperature profiles.
4. Axial momentum change is important, particularly at higher temperature ratios. The effect, which is almost independent of the value of Reynolds number, is to decrease the value of the pressure drop coefficient. At low Reynolds numbers with high temperature ratios there is a need for fuller analysis in which allowance is made for radial velocity.
5. Axial conduction becomes of increasing importance as the Reynolds number is reduced below 200.
6. Free convection causes appreciable increase in the value of the pressure drop coefficient.
7. Reversal of flow near the wall occurs at lower values of Gr/Re than in the uniform property solution.

REFERENCES

1. S. D. POISSON, *Théorie Mathématique de la Chaleur*. Bachelier, Paris (1835).
2. T. B. DREW, Mathematical attacks on forced convection problems: a review, *Trans. Amer. Inst. Chem. Engrs* **26**, 26 (1931).
3. J. R. SELLARS, M. TRIBUS and J. S. KLEIN, Heat transfer to laminar flow in a round tube or flat conduit—The Graetz problem extended, *Trans. Amer. Soc. Mech. Engrs* **78**, 441 (1956).

4. A. P. COLBURN, A method of correlating forced convection heat-transfer data and a comparison with fluid friction, *Trans. Amer. Inst. Chem. Engrs* **29**, 174 (1933).
5. R. L. PIGFORD, Nonisothermal flow and heat transfer inside vertical tubes, *Chem. Engng Prog.* Symposium Series No. 17, **51**, 79 (1955).
6. R. G. DEISSLER, Analytical investigation of fully developed laminar flow in tubes with heat transfer with fluid properties variable along the radius, *NACA* Technical Note 2410 (1951).
7. T. M. HALLMAN, Experimental study of combined forced and free laminar convection in a vertical tube, *NASA* Technical Note *D*-1104 (1961).
8. G. A. OSTROUMOV, *Syobodnaya convectzia v ousloviakh vnoutrennei zadachi* State Publishing House, Moscow (1952). (Translated as *NACA TM* 1407, Free convection under the conditions of the internal problem, 1958.)
9. T. M. HALLMAN, Combined forced and free laminar heat transfer in vertical tubes with uniform internal heat generation, *Trans. Amer. Soc. Mech. Engrs* **78**, 1831 (1956).
10. T. J. HANRATTY, E. M. ROSEN and R. L. KABEL, Effect of heat transfer on flow field at low Reynolds numbers in vertical tubes, *Ind. & Eng. Chem.* **50**, 815 (1958).
11. G. F. SCHEELE, E. M. ROSEN and T. J. HANRATTY, Effect of natural convection on transition to turbulence in vertical pipes, *Canad. J. Chem. Engng* **38**, 67 (1960).
12. S. N. SINGH, Heat transfer by laminar flow in a cylindrical tube, *App. Sci. Res., Sec. A*, **7**, 325 (1958).
13. B. S. PETUKHOV and F. F. TSVETKOV, Raschet reploobmena pri laminarnom techenii zhidkosti v trubakh v oblasti malykh chisel pecle (Calculation of heat exchange under conditions of laminar flow of fluids in tubes over a range of small Peclet numbers.) *Inzh. Fiz. Zh.* **4**, 10 (1961).
14. E. R. G. ECKERT and R. M. DRAKE, *Heat and Mass Transfer*. McGraw-Hill, London (1959).
15. J. HILSENRATH, Tables of thermal properties of gases, U.S. Dep. of Commerce Nat. Bureau of Standards Circular 564, Washington (1955).
16. J. G. KNUDSEN and D. L. KATZ, *Fluid Dynamics and Heat Transfer*, p. 435. McGraw-Hill, London (1958).
17. W. M. KAYS and W. P. NICOLL, Laminar flow heat transfer to a gas with large temperature differences, *J. Heat Transfer* **85**, Series C, 329 (1963).
18. B. S. PETUKHOV and A. YA. YUSHIN, Heat exchange during liquid metal flow in the laminar and transition regions, *Sov. Phys.-Dokl.* **6**, 159 (1961).
19. G. F. SCHEELE and T. J. HANRATTY, Effect of natural convection on stability of flow in a vertical pipe, *J. Fluid Mech.* **14**, 244 (1962).

APPENDIX I

The use of Simpson's rule in the computer programme

The necessary integrations with respect to radius were carried out by the use of Simpson's rule. A check on errors due to the use of increments of radius which were too large was obtained from the velocity and temperature profiles. The mixed mean temperature was derived from these and the value compared with the original "imposed" value. Discrepancies not disappearing on further iteration were remedied by the use of smaller increments of radius.

Evaluations at the following radii were found to give satisfactory accuracy: R from 0 by increments of 0·05 to 0·9, 0·925, 0·95, 0·9625, 0·975, 0·9875, 1·000. The smaller increments close to the wall were necessary because of the steeper gradients.

Résumé—L'effet de la variation de la chaleur spécifique, de la densité, de la viscosité et de la conductivité thermique avec la température, est recherché théoriquement pour un écoulement d'air réfrigérant développé dans un tube circulaire. Des solutions numériques sont présentées qui ont été obtenues à l'aide d'un calculateur numérique et dans une gamme de températures de 350 à 2500°K.

Les équations de quantité de mouvement et de l'énergie sont considérées et les solutions numériques des profils de température et de vitesse, le nombre de Nusselt et le coefficient de chute de pression sont donnés pour différentes températures moyennes.

Des solutions sont présentées pour les conditions de: 1—Tous les gradients axiaux de température à rayon fixé égaux au gradient de température globale. 2—Température pariétale constante.

En plus de montrer les effets de la variation des propriétés, les solutions montrent aussi que l'effet de la conduction axiale devient important aux faibles nombres de Reynolds et que l'effet du changement de la quantité de mouvement axiale peut être considérable pour de grandes différences de température entre l'air et la paroi. Pour un écoulement vertical ascendant, l'effet de la force de gravitation est étudié et la solution numérique indique un renversement de l'écoulement près de la paroi à une valeur plus faible de Gr/Re que dans la solution avec propriétés uniformes.

Zusammenfassung—Der Einfluss der Änderung der spezifischen Wärmekapazität der Dichte, der Zähigkeit und der Wärmeleitfähigkeit mit der Temperatur wird theoretisch für einen ausgebildeten Luftstrom, der in einem Rohr mit Kreisquerschnitt kühlt, untersucht. Es werden numerische Lösungen

angegeben, die mit einem Digitalrechner erzielt wurden und für einen Bereich der Lufttemperaturen von 350 bis 2500°K gelten. Die Impuls- und Energiegleichungen werden berücksichtigt und für unterschiedliche mittlere Temperaturen werden numerische Lösungen der Temperatur- und Geschwindigkeitsprofile, Nusseltzahl und Druckabfallbeiwert angegeben.

Es werden Lösungen aufgeführt für die Bedingungen, dass:

1. alle axialen Temperaturgradienten bei einem bestimmten Radius dem Gradienten der Mischtemperatur gleich sind
2. konstante Wandtemperatur vorliegt.

Zusätzlich zum gezeigten Einfluss der Stoffwertevariation ergeben die Lösungen auch, dass der Einfluss der axialen Leitung bei niedrigen Reynoldszahlen an Bedeutung gewinnt und dass bei grossen Temperaturunterschieden zwischen Luft und Wand der Einfluss der Axialimpulsänderung beträchtlich sein kann. Für senkrechte Aufwärtsströmung wird der Einfluss der Schwerkraft untersucht und die numerische Lösung zeigt einen Umkehrstrom in Wandnähe bei niedrigeren Werten von Gr/Re als es bei der einheitlichen Lösung für die Stoffeigenschaften der Fall ist.

Аннотация—Теоретически исследуется влияние изменения теплоёмкости, плотности, вязкости и теплопроводности с температурой при охлаждении развитого потока воздуха в круглой трубе. Приведены численные результаты для диапазона температур воздуха от 350 до 2500°К, полученные на цифровой вычислительной машине.

Рассмотрены уравнения количества движения и энергии и приведены численные результаты для профилей температуры и скорости, критерий Нуссельта и коэффициент перепада давления для различных смешанных средних температур.

Решения представлены для следующих условий:

1. Все аксиальные градиенты температуры при фиксированном радиусе равны градиенту среднеобъёмной температуры.
2. Постоянная температура стенки.

Помимо того, что решения указывают на влияние изменения свойств, они также показывают, что влияние продольной теплопроводности становится важным при малых значениях критерия Рейнольдса, а влияние аксиального изменения количества движения может быть значительным при большой разности температур между воздухом и стенкой.

Изучается влияние гравитационной силы для потока, направленного вертикально вверх. Численное решение указывает на перемену направления потока у стенки при меньшем значении величины Gr/Re, чем в решении с однородными свойствами.